

Reversal mechanisms and interactions in magnetic systems: coercivity versus switching field and thermally assisted demagnetization

F. CEBOLLADA,^{A)} J.M. GONZÁLEZ,^{B)} J. DE FRUTOS^{C)} AND A.M. GONZÁLEZ^{A)}

^{A)}Departamento de Física Aplicada a las Tecnologías de la Información, EUIT de Telecomunicación, Universidad Politécnica de Madrid, Cra. de Valencia, Km 7, 28031 Madrid, Spain.

^{B)}Instituto de Ciencia de Materiales de Madrid - CSIC, 28049 Cantoblanco, Madrid, Spain, and Instituto de Magnetismo Aplicado, RENFE-UCM, Pinar de las Rozas, Madrid, Spain.

^{C)}Departamento de Física Aplicada a las Tecnologías de la Información, ETSI de Telecomunicación, Universidad Politécnica de Madrid, Ciudad Universitaria s/n, 28040 Madrid, Spain

In this paper we present a comparative analysis of the magnetic interactions and reversal mechanisms of two different systems: NdFeB-type alloys with grain sizes in the single domain range and Fe-SiO₂ nanocomposites with Fe concentrations above and below the percolation threshold. We evidence that the use of the coercivity as the main parameter to analyse them might be misleading due to the convolution of both reversible and irreversible magnetization variations. We show that the switching field and thermally assisted demagnetization allow a better understanding of these mechanisms since they involve just irreversible magnetization changes. Specifically, the experimental analysis of the coercivity acquisition process for the NdFeB-type system suggests that the magnetization reversal is nucleated at the spin misalignments present due to intergranular exchange interactions. On the other hand, the study of the magnetic viscosity and of the isothermal remanent magnetization (IRM) and direct field demagnetization (DCD) remanence curves indicates that the dipolar interactions are responsible for the propagation of the switching started at individual particles.

Keywords: magnetization reversal, coercivity, switching field distribution, magnetic interactions, magnetic viscosity.

Mecanismos de inversión de la magnetización e interacciones en sistemas magnéticos: campo coercitivo versus campo de conmutación y desimantación térmicamente asistida

En este artículo presentamos un análisis comparativo de la influencia de la microestructura a través de las interacciones magnéticas en los mecanismos de inversión de la magnetización en dos sistemas diferentes: aleaciones tipo NdFeB con tamaños de grano en el rango de monodominio y nanocompuestos de Fe-SiO₂ con concentraciones de Fe tanto por encima como por debajo del umbral de percolación. Ponemos de manifiesto que el uso del campo coercitivo como parámetro de análisis puede llevar a equívocos debido a la coexistencia de variaciones reversibles e irreversibles de la magnetización. También mostramos que el campo de conmutación y la desimantación térmicamente asistida permiten una mejor comprensión de dichos mecanismos ya que reflejan exclusivamente cambios irreversibles de imanación. Concretamente, el análisis experimental del proceso de adquisición de coercitividad de los sistemas tipo NdFeB sugiere que la inversión de la magnetización se nuclea en los desalineamientos de los espines debidos a las interacciones de canje intergranular en las fronteras de grano. Por otra parte, el estudio de la viscosidad magnética y de las curvas de remanencia isoterma (IRM) y de remanencia de desimantación DC (DCD) de los nanocompuestos de Fe-SiO₂ indica que las interacciones dipolares son responsables en este sistema de la propagación de la conmutación, que se genera en partículas individualmente consideradas.

Palabras clave: inversión de la magnetización, coercitividad, distribución de campos de conmutación, interacciones magnéticas, viscosidad magnética.

1. INTRODUCTION

The hysteresis (extrinsic) properties of magnetic materials are strongly dependent on their particular microstructures. The improvement and versatility of preparation techniques in the last decades have allowed the production of many types of high quality magnetic materials, ranging from metallic systems to different oxides, usually with very well controlled morphological and structural features, even down to a nanoscopic scale. Among these techniques are ultrarapid quenching, sputtering, molecular beam epitaxy, pulsed laser deposition, etc. New phenomenology has emerged from these materials, due a combination of factors such as reduced dimensionality (size and surface effects) and interphase coupling: oscillatory exchange coupling in multilayers, spin-dependent scattering effects in multilayers and granular

systems, colossal magnetoresistance, exchange bias across ferro-antiferromagnetic interfaces, enhanced soft behaviour of nanocrystalline alloys and hard behaviour of the so-called spring magnets, giant coercivity of nanoparticulated systems and configurational anisotropy in nanoelements (1). From a technological point of view, new devices are springing associated to this phenomenology, related to magnetic recording, spintronics (the control of electron current through spin), magneto-electromechanical systems... (2)

One of the main problems for the control of the extrinsic properties of these new materials lies in the preponderant role of the magnetic interactions either in their relaxation behaviour and/or in their hysteresis processes. Exchange (short ranged) and dipolar (long range) interactions compete

in a multiscale problem involving structural features in a broad range of lengths. The analysis of magnetic interactions is still a challenging problem due to several factors: (i) the lack of measurement techniques or probes to analyze the values of the relevant magnetic energies -mainly exchange, anisotropy and magnetoelastic- in local environments that can be very different from those of bulk phases (e.g. surfaces, grain boundaries or interfaces), and that are responsible in many occasions for the start of the magnetization reversal; (ii) the absence of simple predictive theories or models to take into account the influence of interactions on the magnetization and relaxation processes; (iii) there are no easy-to-interpret experimental procedures that can yield direct values of the strength of the interactions.

In a general scheme, the effect of the interactions on the behaviour of magnetic systems can be assessed through their field-dependent magnetization processes (hysteresis) and through their thermally assisted magnetization-demagnetization processes (3, 4). In the case of the hysteresis processes, the interactions may just modify the field sensed by the regions that trigger the switching of the magnetization without affecting the reversal mode in itself, although in many cases they also modify the magnetization switching mode, leading to mechanisms that require an entirely new approach for their analysis. In most cases the interactions cannot be treated in the basis of a mean field approach, this being specially true when the reversal starts from highly localized regions of the samples or when the reversal mode is modified by the interactions. The thermally-assisted magnetization-demagnetization, as a general idea, yields the range of energies (involved in the reversal of the regions where the switching starts) that are accessible to thermal fluctuations along a given time window (5). The lapse of this time window may vary from thousands of seconds -for conventional DC magnetization measurements- to even picoseconds for some spectroscopic techniques. However, and according to the assertions of the previous paragraph, the lack of general experimental routines to directly measure interactions compels us to design the specific measurement strategy in order to evaluate them, depending on the particular features of the samples under study or the experimental techniques available.

In this paper we present a comparison of the analysis of the magnetic interactions in two systems with different characteristic structural lengths and reversal mechanisms, by using techniques related to their hysteresis mechanisms (remanence curves and similar) and thermally-assisted demagnetization. We will show first the analysis of a series of samples consisting of Fe nanoparticles embedded in silica, with concentrations above and below the percolation threshold. Then we will present results on the coercivity acquisition of a set of NdFeB-type alloys with grain sizes in the single domain range.

2. Fe-SiO₂ SYSTEM

The magnetism of nanoparticles is extremely complex due to a combination of factors. First, the breaking of the local symmetry at the surface, which represents a significant percentage of the total particle mass, may give rise to phenomena such as spin canting or modified local anisotropy (6). Second, size effects may also become important, specially for particle sizes of the order of the exchange or magnetostatic correlation lengths, leading to highly inhomogeneous

magnetization distributions inside the particles or to modified spin-wave spectra. Third, magnetic interactions -dependent on the specific particle shape and size distribution, as well as on the degree of dispersion of the particles- greatly influence the hysteresis processes of particulate systems (7).

In the case of Fe_x(SiO₂)_{1-x} nanocomposites, x being the volume concentration, most authors have reported high coercivities, well above the maximum theoretical values associated to switching through coherent rotation (about 180 Oe for an isotropic distribution of particles), even up to about 1.5 kOe at room temperature. The maximum coercivity for most batches of samples takes place at concentrations about x=0.3-0.4, sharply decreasing for higher concentrations, and it cannot usually be correlated with parameters such as the variation of particle size or shape with concentration (8-10). This suggests that (dipolar) interactions play a fundamental role in the magnetization process of this type of composites.

2.1 Experimental

We present some results on the effects of the interactions in a series of Fe_x(SiO₂)_{1-x} nanocomposites, prepared by ball milling with concentrations in the range x=0.2-0.6. The average grain size of the particles, as evaluated through XRD, is 18 nm almost independent of the concentration and milling time. Transmission electron microscopy (TEM) studies revealed the existence of a broad particle size distribution, ranging from a few nanometers to about 40 nm, in all samples. They also showed that particle clusters are more frequent in those samples with concentrations x=0.5 and 0.6, as expected. The magnetic studies, carried out in an EG&G vibrating sample magnetometer (VSM) under maximum applied fields of 1T, showed a maximum in the coercivity and in the remanence-to-saturation ratio for x=0.3 (Figure 1). The maximum coercivity, 380 Oe, is well above the coherent rotation value (11), in agreement with most reports in the literature.

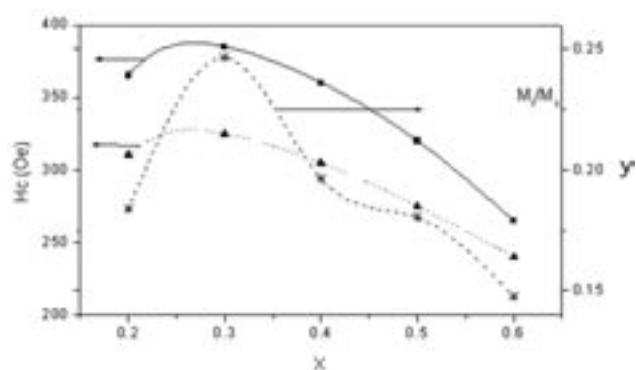


Fig. 1.- Concentration dependence of the coercivity for the 60 h milled (squares) and 48 h milled (triangles) samples, and of the reduced remanence (stars) for the 60 h milled sample.

The fact that the coercivity of this set of samples cannot be correlated with parameters such as grain size or shape lead us to analyse the role of magnetic (dipolar) interactions in their switching mechanisms. This we did by comparing the magnetic viscosity and irreversible processes corresponding either to the virgin (first) magnetization curve and to the demagnetization curve. In order to separate the reversible

processes from the irreversible, remanence curves were used due to the fact that upon application and subsequent removal of a given field only irreversible changes in the magnetization are measured. More specifically, the well known Isothermal Remanent Magnetization (IRM) and DC Demagnetization remanence (DCD) curves were employed to measure the “sign” and intensity of the interactions (12). The IRM plots result from the measurement of the remanence $M_r(H)$ upon application and removal of a field H in a previously demagnetized sample and goes from 0 to $M_{r,max}$; H_m is the field required to reach the maximum remanence while $H_{1/2}$ is the magnetization process mean switching field, i.e. the field required to achieve half the maximum remanence. The DCD curves also result from remanence measurements but by starting from a previously saturated state and applying negative fields, M_r thus varying from $+M_{r,max}$ to $-M_{r,max}$; in this process $H'_{1/2}$ (absolute value) is the mean switching field, i.e. the field required to get null remanence (switching 50% of the sample). It is important to note that the mean switching field is the equivalent to the coercivity when just irreversible processes are considered, in contrast to the “conventional” coercivity, which includes both reversible and irreversible magnetization processes. From these curves, the irreversible susceptibility χ_{irr} and switching field distribution SFD can be calculated as

$$\chi_{irr} = dM_r(H) / dH, \tag{1}$$

$$SFD = d[M_r / M_{r,max}] / dH \text{ (magnetization)} \tag{2a}$$

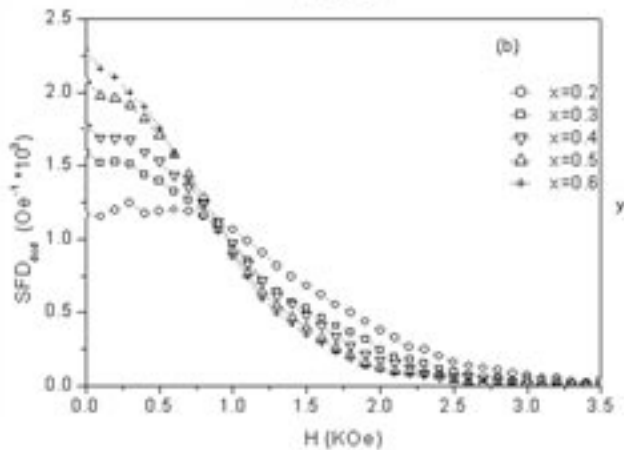
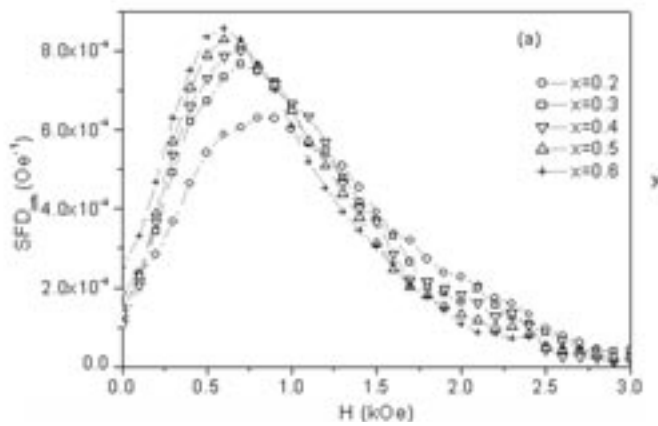


Fig. 2.- Switching field distributions for the magnetization (a) and demagnetization (b) processes.

and

$$SFD = d[M_r / 2M_{r,max}] / dH \text{ (demagnetization)}, \tag{2b}$$

and the ΔM plots can be obtained from the equation

$$\Delta M(H) = m_{DCD}(H) - [1 - 2m_{IRM}(H)] \tag{3}$$

where m_{IRM} (m_{DCD}) is the IRM (DCD) remanent magnetization for a given field H , normalised to $M_{r,max}$. Positive (negative) ΔM values indicate that the magnetization process from an initially demagnetized state is softer (harder) than the demagnetization from saturation, which is usually associated with magnetizing (demagnetizing) interactions.

The SFDs corresponding to the magnetization process from the demagnetized state, shown in Figure 2(a), evidence broad distributions with a long tail up to almost 3 kOe. An important feature is that very large fields are required to switch most of the particles: the peaks of the distributions vary between 610 and 820 Oe and mean switching fields $H_{1/2}$ about 1 kOe were obtained. The width of the distributions and $H_{1/2}$ increase with decreasing concentration (Figure 3), in

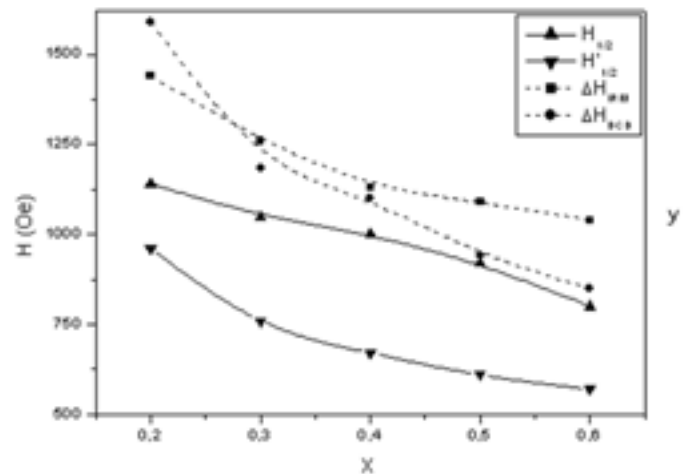


Fig. 3.- Mean switching fields for the magnetization ($H_{1/2}$) and demagnetization ($H'_{1/2}$) processes, as a function of concentration; peak widths, also as a function of concentration, for the magnetization (ΔH_{IRM}) and demagnetization (ΔH_{DCD}) processes, respectively.

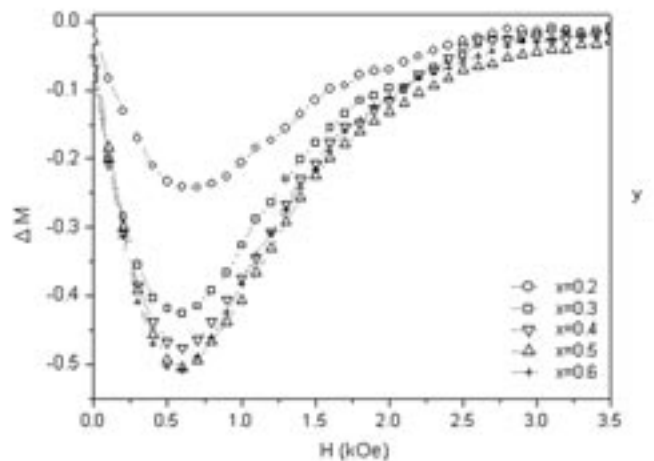


Fig. 4.- ΔM curves for the different samples.

contrast to the maximum coercivity being obtained at $x=0.3$. The SFDs corresponding to the demagnetization process, as it can be seen in Figure 2(b), exhibit basically the same features but shifted to lower fields, as evidenced by the lower values of the mean switching fields $H'_{1/2}$. The only noticeable difference is that the demagnetization starts practically from null fields, which suggest the presence of strong local demagnetizing fields at remanence. As a general idea, no qualitative changes with concentration x are observable in both SFD types, which suggests that there is no change in the switching mechanism for concentrations near the percolation threshold ($x_p \sim 0.5$). The ΔM curves, obtained from the remanence curves, are presented in Figure 4 and evidence negative (demagnetizing) interactions whose intensity increase with concentration, as expected. Again, no qualitative differences are observed for concentrations, respectively, below and above the percolation threshold.

In order to gain insight into the switching mechanism, the magnetic viscosity S of the samples was analysed along both the magnetization and demagnetization processes. Magnetic viscosity can be obtained from the evolution of magnetization with time at constant applied field as:

$$S = -dM/d[\text{Lnt}] \tag{4}$$

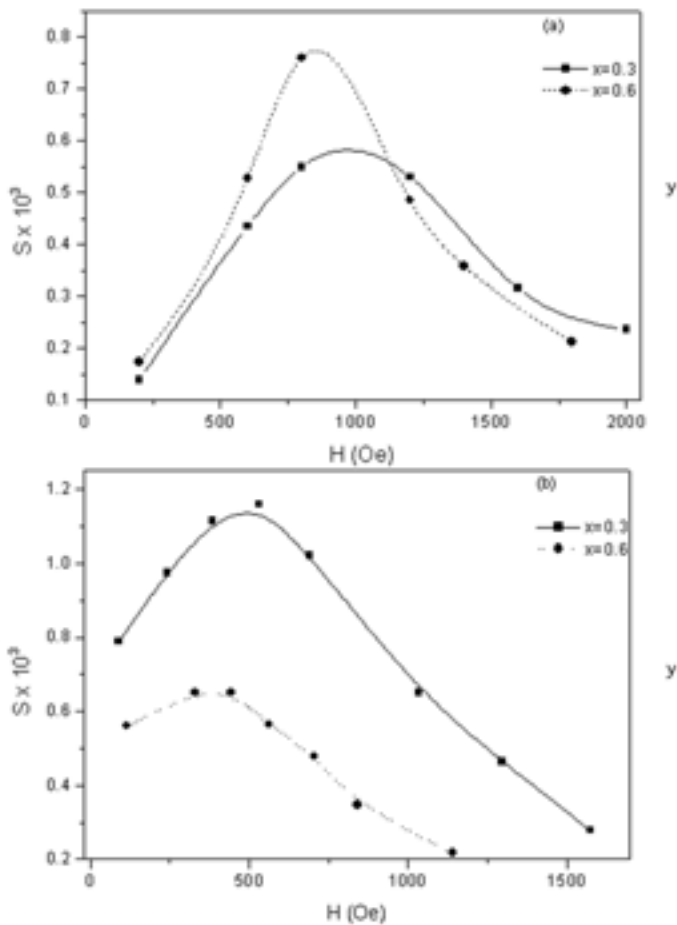


Fig. 5.- Viscosity as a function of the applied field for the samples with $x=0.3$ and $x=0.6$, for the magnetization (a) and demagnetization (b) processes, respectively.

The activation volume v_a corresponds to the volume of the regions of the sample that are susceptible of being reversed by means of thermal fluctuations, in the time window defined in the experiment (in this case, the measuring lapse of time, about 2000 s). In other terms, it is a measure of the energy barriers involved in the reversal mechanism, by considering that this energy is somewhat proportional to the activation volume times the effective anisotropy in that region. The activation volume can be calculated from the following expression

$$V_a = k_B T \chi_{irr} / \mu_0 S_{max} M_s \tag{5}$$

where S_{max} is the maximum viscosity of a given sample (5).

Figure 5 shows the field dependence of the viscosity for the $x=0.3$ and $x=0.6$ samples, for the magnetization (a) and demagnetization processes (b). From the figure it is evident that the maximum viscosity occurs at fields very close to their respective mean switching fields, $H_{1/2}$ and $H'_{1/2}$. The activation volumes calculated from these curves yield particle diameters that are in the range from 15 to 18 nm, which are very close to the grain size obtained from the XRD data.

2.2 Discussion

In this work we have studied the switching mechanisms of a set of Fe-SiO₂ nanocomposites. Although the coercivity exhibits a maximum at $x=0.3$, it cannot be correlated with any observed variation of particle size or shape or any other parameter in our samples; in fact many authors have observed a maximum at similar concentrations in sets of particles characterized by narrow size distributions of equiaxed particles (8-10). We must point out that the coercivity, taken as the field (absolute value) required to attain null magnetization in a previously saturated sample, is not a suitable parameter to analyse in detail the (irreversible) switching mechanisms because it involves both reversible and irreversible magnetization variations. We believe that the analysis of the irreversibilities is a more significant approach, from the point of view of the switching mechanisms. In particular, the “real” coercivity of our samples -evaluated through the mean switching fields $H_{1/2}$ and $H'_{1/2}$ - evidences a monotonic increase with decreasing concentration, which shows that the maximum coercivity at $x=0.3$ is an artefact that is not relevant for the analysis of their reversal mechanisms. In addition to this, the narrower SFDs for high Fe concentrations indicate that a higher percentage of the particles reverse their magnetization in a coupled way for these concentrations. From these data it is apparent that the reversal mechanism is specifically ruled by the magnetic (dipolar) interactions. The analysis of the SFDs and ΔM curves have evidenced that it is harder to magnetize a demagnetized sample than a previously magnetized sample. This can be due to the tendency of the particles to form closed flux structures; these structures, present in the demagnetized state, are difficult to break and lead to high switching fields (note that the magnetization SFDs are almost null for $H=0$). On the other hand, when coming back to zero field from a saturated state, the spontaneous tendency to form closed structures even at zero or very low negative fields makes the demagnetization of the samples very easy and explains why the demagnetization SFDs present maxima close to $H=0$. To complete this picture, the size of the regions involved in the triggering of the reversal process -calculated from viscosity measurements- is very close to the mean particle size. This suggests that although the

dipolar interactions may propagate the reversal of groups of coupled particles, it is started for individual particles.

3. NdFeB-TYPE ALLOYS

3.1 Coercivity acquisition process

NdFeB-type alloys are hard magnets based on the $R_2Fe_{14}B$ phases ($R = Nd, Pr, Dy, \text{etc.}$) with anisotropy fields of the order of 10 T. Suitable microstructures in these magnets yield coercivities well above 1 T, leading to the most successful family of hard magnets in the last two decades (13). Many of these alloys, with grain sizes in the range from tens of nanometers to a few microns, present magnetization curves from the

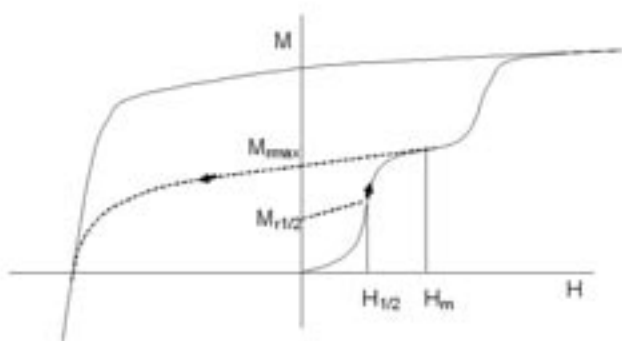


Fig. 6.- Sketch of the virgin magnetization curve of a NdFeB-type magnet, showing two high susceptibility steps.

demagnetized state (virgin curves) that are characterized by two high susceptibility steps, the first one occurring at low fields, and the second one at high fields, close to the (absolute) value of the critical field (the field at which the maximum of the susceptibility takes place in the demagnetization curve) (14). Fig. 6 shows a sketch of a typical magnetization curve; for fields above H_m all the "soft" grains involved in the first reversal step are now coercive and, if the field is reversed back from H_m , values close to the critical field are required to switch their magnetization (dotted curve in Fig. 6).

(i) homogeneous environment

The remanence $M_{r,max}$ measured after taking the field to H_m in the virgin curve represents that of the initially soft grains, i.e. those involved in the first magnetization step. The field $H_{1/2}$

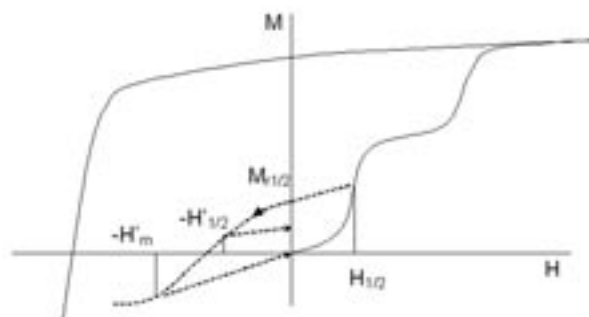


Fig. 7.- Sketch of the coercivity acquisition process in an inhomogeneous environment.

is the field required to -starting from the demagnetized state- reach a remanence $M_{r1/2} = M_{r,max}/2$, that is to make coercive 50% of the grains involved in the first step. This coercivity acquisition process takes place in a more or less homogeneous environment, with the average magnetization pointing in the positive direction, except for those grains that were already coercive (those involved in the second magnetization step, whose average magnetization is still null).

(ii) inhomogeneous environment

Starting from $M_{r1/2}$, i.e. with 50% of the initially soft grains already coercive, we apply negative fields, as shown in Fig. 7. After applying a field $-H'_{1/2}$ and removing the field a remanence equal to $M_{r1/2}$ is obtained, which indicates that we have reversed 50% of the yet soft grains (i.e. 25% of the initially soft grains). If the applied field, starting again from $M_{r1/2}$, is H'_m the remanence after removing the field is now null. H'_m is the field required to make coercive all the remaining soft grains (50% of the initially soft grains). The difference is that in this process we have been dealing with low magnetization, about zero, this reflecting an inhomogeneous environment, with many grains pointing in either positive and negative direction.

TABLE I. "SAMPLES" COMPOSITION AND PREPARATION PARAMETERS

Sample	Composition	Preparation	Anneal
A	$Nd_{13.6}Dy_{2.4}Fe_{76}B_8$	Mechanical Alloying	700°C, 30 min
B	$Nd_{12}Dy_3Fe_{76}B_9$	Melt spinning	700°C, 30 min
C	$Nd_9Pr_6Fe_{76}B_9$	Melt spinning	-
D	$Nd_6Pr_9Fe_{76}B_9$	Melt spinning	580°C, 15 min

TABLE II. COMPARISON OF THE FIELDS REQUIRED TO REVERSE 50% OF THE GRAINS IN A HOMOGENEOUS ($H_{1/2}$) AND INHOMOGENEOUS ($H'_{1/2}$) ENVIRONMENT IN ISOTROPIC AND ORIENTED SAMPLES (14), BOTH IN T AND REDUCED TO THEIR RESPECTIVE SATURATION MAGNETIZATION VALUES.

Sample	Composition	μM_s (T)	$\mu H_{1/2}$ (T)	$\mu H'_{1/2}$ (T)	$H_{1/2} / M_s$	$H'_{1/2} / M_s$
A (iso)	$Nd_{13.6}Dy_{2.4}Fe_{76}B_8$	1.47	0.34	0.76	0.23	0.52
B (iso)	$Nd_{12}Dy_3Fe_{76}B_9$	1.24	0.3	0.83	0.25	0.69
C (iso)	$Nd_9Pr_6Fe_{76}B_9$	1.55	0.4	0.95	0.26	0.61
D (iso)	$Nd_6Pr_9Fe_{76}B_9$	1.5	0.4	0.8	0.27	0.53
OR1*	$Pr_{17}Fe_{75}B_8$	1.29	0.61	1.93	0.47	1.5
OR2*	$Pr_{17}Fe_{75}B_8$	0.45	0.8	1.8	1.77	4
OR3*	NdFeB	1.29	0.87	1.89	0.67	1.47
OR4*	NdFeBV	1.29	0.75	2.05	0.58	1.59

3.2 Experimental results and discussion

Our samples were prepared by out-of-equilibrium techniques (mechanical alloying and melt spinning) and submitted to thermal annealing to crystallize them (except sample C, that was already crystalline in the as-quenched state). Table 1 shows the compositions and preparation parameters of all of them. The microstructure of all samples was characterized by an homogeneous isotropic distribution of grains of the hard 2:14:1 phase with sizes of about 150-200 nm, well below the single domain size for these alloys (15), as evidenced through XRD and SEM studies. In all cases the percentage of grains with sizes above about 400 nm is less than 5%.

The virgin and demagnetization curves were measured in an induction device based on a 12 T superconducting coil and, as it can be seen in Fig. 8, exhibit the low field, high susceptibility region. By following the measurement procedures to analyse the acquisition of coercivity already described for either a homogeneous or inhomogeneous environment, the fields $H_{1/2}$ and $H'_{1/2}$ were obtained. Table 2 shows values of the saturation magnetization, of $H_{1/2}$ and $H'_{1/2}$ and of $H_{1/2}$ and $H'_{1/2}$ normalized to M_s , for our samples and for a set of oriented samples from other authors (14), prepared by sintering and with grain sizes of the order of 1 μm . As it can be seen, quite homogeneous values are obtained for $H_{1/2}$ and $H'_{1/2}$ for the isotropic samples and also for the oriented ones.

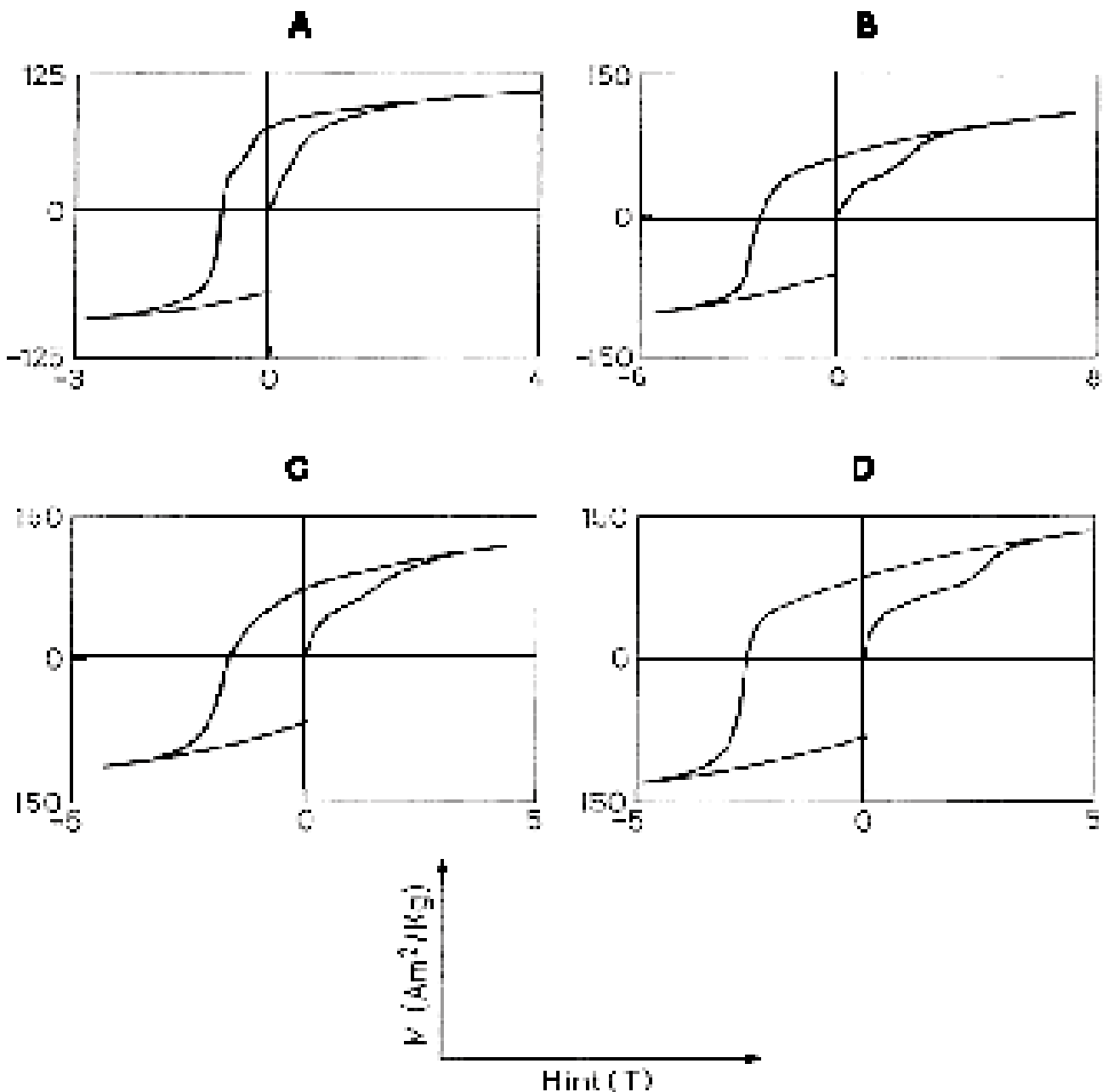


Fig. 8.- Initial magnetization curves and demagnetization curves of NdFeB type samples.

The field required to achieve coercivity in 50% of the grains is about 2 to 3 times larger for an inhomogeneous environment than for a homogeneous one, independent of the samples being isotropic or oriented. However, when comparing isotropic and oriented samples, values systematically twice larger, approximately, are observed for the oriented ones. An important issue is that sample OR2, whose saturation magnetization is really different from the rest of the samples, still presents quite similar values of $H_{1/2}$ and $H'_{1/2}$.

The fact that the acquisition of coercivity is more difficult to achieve in inhomogeneous environments could be explained if we consider that dipolar fields rule this process. In an inhomogeneous environment a large amount of poles and high stray fields are expected, associated with many discontinuities in the magnetization across the grain boundaries. However, in this case we should expect that the values obtained for the isotropic environment are larger than those of the oriented ones, which is not the case. In addition to it, it is obvious that sample OR2 shows that the field required to achieve coercivity can not be correlated with the saturation magnetization; this sample, with an excess B content, has a saturation magnetization that is roughly one third that of the rest of the samples, but it still has similar $H_{1/2}$ and $H'_{1/2}$ values. This leads us to believe that the dipolar fields, although they must be present and contribute to the internal field sensed by the grains during the coercivity acquisition process, do not rule the coercivity acquisition process, i.e. a different mechanism must be responsible for the reversal of the grains.

The role of exchange coupling across the grain boundaries in the magnetization-demagnetization process of NdFeB and similar alloys has been the object of a lot of works, many of them devoted to simulation, and it is considered to lie in the origin of the fact that the field required to switch their magnetization is one order of magnitude below the initially expected value, i.e. the anisotropy field H_K (16-18). In particular, intergranular exchange coupling becomes extremely important in nanocrystalline (spring) magnets, for which the exchange length (basically the length of a domain wall, which for these magnets is a few nanometers) is of the order of the grain size; this yields a more homogeneous magnetization distribution and, consequently, enhances their remanence, but, as a countereffect, it decreases their coercivity (19).

Regarding intergranular exchange coupling, it is expected to be smaller than the intragranular (bulk) exchange, due to the lattice distortion across the boundary. However, different simulation jobs have evidenced that the wall-like structure appearing at it acts as a "nucleation" site for the magnetization reversal, yielding coercivity values in the correct order of magnitude if the boundary exchange is a few tens percent of the bulk value (16-18). As an example, Figure 9 presents the switching field H_s required to reverse the magnetization of a grain with a neighbouring grain with (initially) antiparallel magnetization, for an intergranular coupling of 80% the bulk value and for different values of the exchange-to-anisotropy ratio. Reasonable values of this ratio are in the order of unity (it is close to 2 for the $\text{Nd}_2\text{Fe}_{14}\text{B}$ phase). Switching field values are in the order of 0.05 to $0.2H_K$. It is important to note that if both grains present parallel magnetization, the switching field (to reverse both) rises again to values about H_K . This intergranular exchange based mechanism (see Fig. 10) accounts

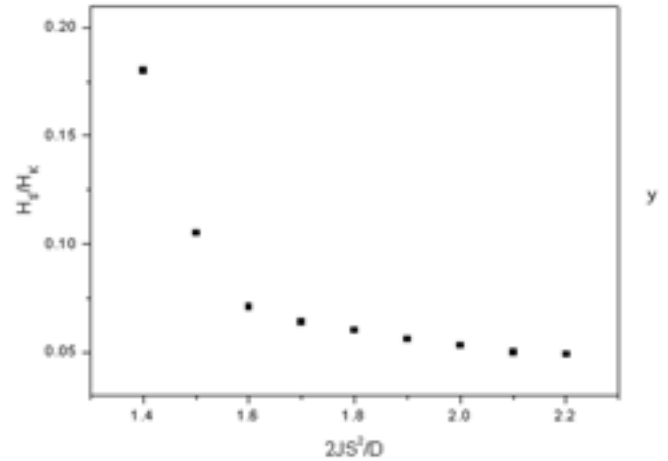


Fig. 9.- Reduced switching field as a function of the exchange-to-anisotropy ratio for an intergranular exchange coupling equal to 80% the bulk value.

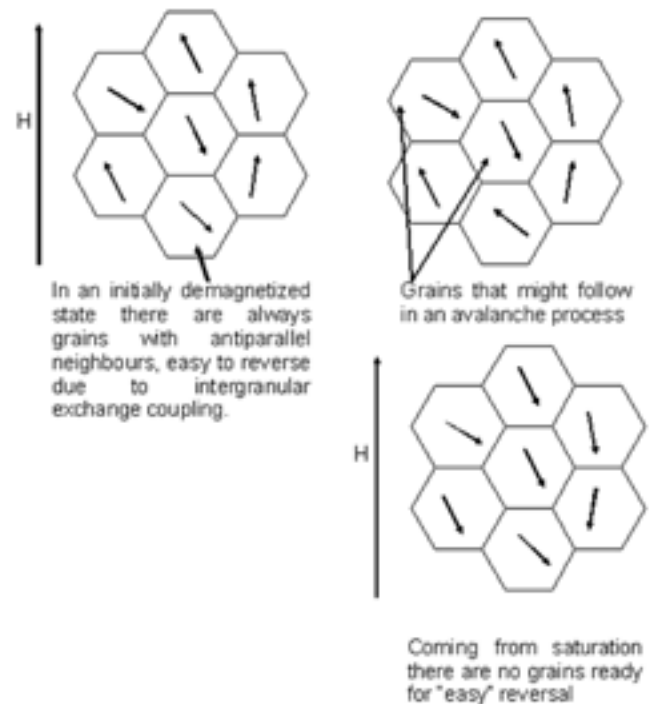


Fig. 10.- Model of magnetization and demagnetization processes of NdFeB type alloys, based on avalanches due to intergranular exchange coupling.

for the main features of the magnetization and demagnetization process: in an initially demagnetized sample there are always grains with antiparallel neighbours that can be reversed at low fields, leading to an avalanche process. If the reversal is not complete, the process is more or less reversible; however, if the reversal is fully achieved (e.g. in the demagnetiation of a previously saturated sample) no antiparallel grains are available for triggering a low field reversal.

4. CONCLUSIONS

We have analysed in this paper the role of interactions on the switching mechanisms of two types of magnets ruled, respectively, by dipolar and intergranular-exchange interactions. In both cases a strategy was used based on the comparison of the evolution of the magnetization and demagnetization processes with a variable parameter, Fe concentration and M_s for the Fe-SiO₂ composites and the NdFeB-type magnets, respectively. We have also shown that, from the point of view of the switching mechanisms the SFDs, obtained from remanence measurements, are clearly more significant than coercivity.

In the particular case of the Fe-SiO₂ composites, our results clearly suggest that closed flux structures present in the demagnetized state are responsible for the high switching fields required to magnetize the samples. The reversal in these samples is triggered by individual particles and propagated by dipolar interactions, irrespectively of the Fe concentration being either above or below the percolation threshold. In the case of the NdFeB-type magnets, we have shown that intergranular exchange accounts for most of the features observed in the high susceptibility regions of demagnetized samples as well as for the higher fields required to reverse previously saturated samples.

REFERENCES

1. Science and Technology of Nanostructured Magnetic Materials. G.C. Hadjipanayis and G.A. Prinz (eds.), Plenum Press, New York, 1991.
2. G.A. Prinz. "Magnetoelectronic applications," *J. Magn. Magn. Mater.* 200, 57-68 (1999).
3. J.M. González, A. Salcedo, F.J. Palomares, F. Cebollada, C. Prados and A. Hernando, "Crossover from local to collective magnetic relaxation modes in Co/Ni multilayers," *J. Magn. Magn. Mater.* 242-245, 518-520 (2002).
4. M. Alonso-Sañudo, J.J. Blackwell, K. O'Grady, J.M. González, F. Cebollada and M. P. Morales, "Magnetic behaviour and percolation in mechanically alloyed Fe-SiO₂ granular solids," *J. Magn. Magn. Matter.* 221, 207-214 (2000).
5. P. Gaunt, "Magnetic viscosity and thermal activation energy," *J. Appl. Phys.* 59, 4129-4132 (1986).
6. M.P. Morales, S. Veintemillas-Verdaguer, M.I. Montero and C.J. Serna, "Surface and internal spin canting in gamma-Fe₂O₃ nanoparticles," *Chem. Mater.* 11, 3058-3064 (1999).
7. G.C. Hadjipanayis and R.W. Siegel (Eds.), *Nanophase Materials: Synthesis, Properties, Applications* (Kluwer Ac. Publ., Dordrecht, 1994).
8. C.L. Chien. "Granular solids," pp. 477-496 in *Science and Technology of Nanostructured Magnetic Materials*. G.C. Hadjipanayis and G.A. Prinz (eds.), Plenum Press, New York, 1991.
9. C. de Julián, A.K. Giri, M.P. Morales and J.M. González, *Script. Metallurgica Mater.*, "Thermally activated demagnetization in Fe-SiO₂ granular solids," 33, 1709-1716 (1995).
10. J.A. Christodoulides, N.B. Shevchenko, G.C. Hadjipanayis and V. Papaefthymiou, "Effect of preparation conditions on the hysteresis behavior of granular Fe-SiO₂," *J. Magn. Magn. Mater.* 166, 283-289 (1997).
11. I. Joffe and R. Heuberger, "Hysteresis properties of distributions of cubic single-domain ferromagnetic particles," *Phil. Mag.* 314, 1051-1059 (1974).
12. M. El-Hilo, K. O'Grady, T.A. Nguyen, P. Baumgart, and I.L. Sanders, "Interactions in CoPtCr/SiO₂ composite thin films," *IEEE Trans. on Mag.* 29, 3724-3726 (1993).
13. J.M.D. Coey, *Rare-Earth Iron Permanent Magnets* (Clarendon Press, Oxford, 1996).
14. D. Givord, Q. Lu, F.P. Missell, M.F. Rossignol, D.W. Taylor and V. Villas-Boas, "A direct study of the dipolar field in several RFeB systems," *J. Magn. Magn. Mater.* 104-107, 1129-1131 (1992).
15. K. Dürst and H. Kronmüller, "The coercive field of sintered and melt-spun NdFeB magnets," *J. Magn. Magn. Mater.* 59, 86-94 (1986).
16. J.M. González, F. Cebollada and A. Hernando, "Modelling the influence of intergranular phases on the hysteresis behaviour of hard magnetic polycrystals," *J. Appl. Phys.* 73, 6943-6945 (1993).
17. J. Fidler, T. Schrefl, W. Scholz, D. Suess, R. Dittrich and M. Kirschner, "Micromagnetic modelling and magnetization processes," *J. Magn. Magn. Mater.* 272-276, 641-646 (2004).
18. M. Emura, J.M. González, and F.P. Missell, "Magnetization reversal processes linked to interphase exchange and dipolar coupling in hard-soft nanocomposite magnets," *J. Appl. Phys.* 81, 4983-4985 (1997).
19. E.E. Fullerton, J.S. Jiang and S.D. Bader, *J. Magn. Magn. Mater.* "Hard/soft magnetic heterostructures: model exchange-spring magnets," 200, 392-404 (1999).

Recibido: 10.01.05

Aceptado: 07.04.05

